Effect of Different Calcination Temperatures and Carbon Coating on the Characteristics of $LiFePO_4$ Prepared by Hydrothermal Route

Nofrijon Sofyan [#1], Guntur Tri Setiadanu [#2], Anne Zulfia [#3], Evvy Kartini [*4]
[#] Department of Metallurgical and Materials Engineering,
Faculty of Engineering, Universitas Indonesia, Depok 16424, Indonesia
[1] nofrijon.sofyan@ui.ac.id
[2] guntur.setiadanu@gmail.com
[3] anne@metal.ui.ac.id
[*] National Nuclear Agency (BATAN), Kawasan PUSPIPTEK, Serpong, Indonesia
[4] kartini@batan.go.id

***Abstract*—The characteristics of lithium iron phosphate ($LiFePO_4$) prepared via hydrothermal route and calcined at various temperatures have been examined. Calcinations were performed at temperature variations of 500, 600, and 750°C for 5 hours. The properties were characterized through thermal decomposition, structure, morphological and electrical properties. Flake-shaped pure $LiFePO_4$ and $LiFePO_4$/C was successfully synthesized with the addition of 5 wt.% carbon black. The results showed that the addition of carbon effectively protected the material from oxidation and grain growth. The optimum calcination temperature was obtained at 750°C with flake diameter of 80 nm and average length of 427 nm. The measured conductivity of the carbon coated $LiFePO_4$ (2.23 x 10^{-4} S/cm) was much higher than that of the as-synthesized $LiFePO_4$ (5 x 10-7 S/cm). The battery performance was obtained with a stable voltage ranging from 3.3 to 3.4 volts.**

Keyword- Carbon coating. Hydrothermal, $LiFePO_4$, Cathode, Lithium ion battery

I. INTRODUCTION

Lithium ferro phosphate ($LiFePO_4$) has attracted many investigators since the reversibility of intercalation-deintercalation lithium ion in electrochemical process was observed [1], primarily as a promising candidate for lithium ion battery cathode. Many advantages of this material have been reviewed such as low production cost, environmental friendly and high capacity and stability cycle [2].

Despite its many advantageous, however, $LiFePO_4$ also has a drawback in that its electronic conductivity is low, measured only 10^{-9} S/cm [3]. This low electronic conductivity could lead to a low rate capability. Because of that, several approaches have been proposed by many investigators to improve this conductivity, e.g. refining the grain to nanoscale [4], [5], metal doping [6], [7], carbon coating [2], and co-synthesis with carbon in powder metallurgy method [8].

The synthesis routes of $LiFePO_4$ are mainly divided into two categories. The first route is a solid-state reaction, which involves a combination of mechanical alloying and solid reaction at high temperature [9] – [11]. The second route is a wet chemical approach, which involves utilization of chemical reaction solution followed by crystallization. This approach includes sol-gel [12], [13], hydrothermal [14] – [18], and solvothermal [19], [20].

Solid state route has attracted many investigators due to the ease of the process; however, solid state synthesis needs high temperature for sintering process in addition to the impurity problems dominated by Li_3PO_4 and Fe_2O_3 [21]. In the electrochemical reaction during charge-discharge process, the material containing these impurities will degrade and reduce the capacity of the active material [22]. The alternative is to synthesize $LiFePO_4$ by using hydrothermal route, which involves wet chemical process at low temperature followed by purifying process at relatively high temperature. This route has some advantages such as simple process and relatively low crystallization temperature and thus energy consumption [23]. In addition, the impurities could also be controlled during the reaction process [24].

In this work, $LiFePO_4$ was prepared using the hydrothermal route. The characteristics of the material after calcination at various different temperatures are presented. Further, the effect of carbon coating on the $LiFePO_4$ performance in a lithium ion battery cathode is also examined and discussed.

II. EXPERIMENTAL

A. Synthesis of $LiFePO_4$

The synthesis of $LiFePO_4$ was performed via hydrothermal route. The starting materials LiOH, $FeSO_4 \cdot 7H_2O$ and $NH_4H_2PO_4$ were purchased from Merck and were used as precursors with no further treatment. The precursors were weighed in an analytical balance with a molar ratio of Li : Fe : P = 2 : 1 : 1. Lithium hydroxide was dissolve to form 0.05 mole aqueous solution and was mixed with 0.025 mole of $NH_4H_2PO_4$ under magnetic stirrer agitation to form a white suspension. A solution of 0.025 mole $FeSO_4 \cdot 7H_2O$ was added drop wisely into the suspension and stirred for 45 minutes to form a bluish green suspension. This green suspension was quickly transferred into 100 mL Teflon-lined stainless-steel autoclave and was heated at 180°C for 20 hours. The resultant light bluish green precipitation was collected and washed by distilled water for several times and lastly by using deionized water. The precipitates were then dried at 80°C in an oven for 4 hours before further treatment and characterization.

B. Preparation of Carbon Coated $LiFePO_4$

The as-synthesized $LiFePO_4$ powder from previous step was mixed with 5 wt.% carbon black (CB) and the mixture was ball milled until homogenized and labelled as $LiFePO_4$/C. Some of the mixture were analysed using thermal analyser (Shimadzu DTG-60 Simultaneous Measuring Instrument) for thermal decomposition behaviour. The remain $LiFePO_4$/C was subsequently calcined at various temperatures 500, 600 and 750 °C for 5 hours under nitrogen atmosphere. For comparison, the as-synthesized $LiFePO_4$ was also prepared by the same procedure but with no carbon addition and labelled as $LiFePO_4$. X-ray diffraction (XRD, Pan-Analytical) measurements were conducted using Cu-Kα at 2θ 10-70° and the diffractograms were analysed using JCPDS database as a reference. Scanning electron microscope (SEM, FEI Inspect F50) was used to observe particle morphology and size distribution.

C. Battery Preparation

The carbon coated $LiFePO_4$ from the previous step was used for conductivity measurement and was performed using an electrical impedance spectroscopy (EIS, Hioki LCR 3532-50) from 1 gram of the active material prepared in cylindrical pellet with 0.9 cm diameter pressed at 6 MPa. For the electrochemical test, 80 wt.% of the as-prepared $LiFePO_4$ was mixed with carbon black and poly-vinylidene fluoride (PVDF) with a ratio of $LiFePO_4$: CB : PVDF = 80 : 10 : 10 in N-methyl pyrrolidone (NMP) solvent inside a vacuum mixer. The mixture was applied onto an aluminium sheet as a current collector (MTI) and dried. After drying, the sample was hot-rolled and heated in a vacuum oven at 80°C. The battery was prepared in the forms of a coin using an Li metal anode for half-cell and $LiPF_6$ was used as an electrolyte. The cell was then tested through charge/discharge performance using an MTI battery analyser.

III. RESULT AND DISCUSSION

At dissolving process during the initial stage, the following reaction may take place,

$$6\ LiOH_{(l)} + 3\ NH_4H_2PO_{4\ (l)} + 3\ FeSO_4.7\ H_2O_{(l)} \rightarrow$$
$$Li_3PO_{4\ (s)} + Fe_3(PO_4)_{2\ (s)} + 13\ H_2O + 3\ Li^+ + 3\ NH_2^- + 3\ HSO_4^- + 3\ H^+ \quad (1)$$

Visual appearance of the resultant reaction is bluish green suspension as an indication of Li_3PO_4 and $Fe_3(PO_4)_2$. These compounds are metastable and will act as intermediate compounds of $LiFePO_4$. The equimolar of Li_3PO_4 and $Fe_3(PO_4)_2$ is a key factor to obtain pure $LiFePO_4$ formation in the precursor either in a solid state or a wet chemical method and could only be achieved under excessive Li^+ molar condition [25]. In the autoclave, at reaction temperature of 180°C for 20 hours, the initial precursor suspension will react to form amorphous $LiFePO_4$ and $H_2SO_{4\ (l)}$ according to the expected reaction below:

$$Li_3PO_{4\ (s)} + Fe_3(PO_4)_{2\ (s)} + 13\ H_2O + 3\ Li^+ + 3\ NH_2^- + 3\ HSO_4^- + 3\ H^+ \rightarrow$$
$$3\ LiFePO_{4\ (s)} + 3\ H_2SO_4 + 13\ H_2O + 3\ Li^+ + 3\ NH_2^- \quad (2)$$

As can be seen in the reaction, other reaction products Li^+ and NH_2^- excess dissolving in strong acid supernatant $H_2SO_{4\ (l)}$ should be remove through the washing process. The bluish green precipitate of amorphous $LiFePO_4$ was then collected and dried and subsequently was calcined to obtain pure $LiFePO_4$.

The aforementioned reaction behavior could be observed under thermal decomposition. In this work, samples were characterized using a thermogravimetric analyzer at a heating rate of 10°C/minutes from room temperature to 850 °C under nitrogen environment. Visual observation of the results showed that $LiFePO_4$/C has a dark colour, whereas $LiFePO_4$ has red colour as an indication of oxidation. Figure 1 shows thermal behavior curves for both samples.

As can be seen in Fig. 1a, the TG curve of $LiFePO_4$ sample consists of 3 stages. In the first stage, at temperature 60 – 300°C, there is a slight decrease in mass due to water evaporation. This phenomenon is also characterized by an endothermic reaction culminating at 227^0C. Therefore, it is clear that $LiFePO_4$ decomposition would not occur in this temperature range. In the second part, at 325-610^0C, the weight increases

around 3.86% with three exothermic reactions at 348^{0}C, 540^{0}C and 605^{0}C. This reaction is an oxide decomposition of amorphous $LiFe^{II}PO_4$ into $Li_3Fe_2(PO_4)_3$ and Fe_2O_3 [9] according to the following reaction:

$$LiFe^{II}PO_{4\ (amorphous)} + ¼\ O_2 \rightarrow 1/3\ Li_3Fe_2^{III}(PO_4)_3 + 1/6\ Fe_2{}^{III}O_3 \quad (3)$$

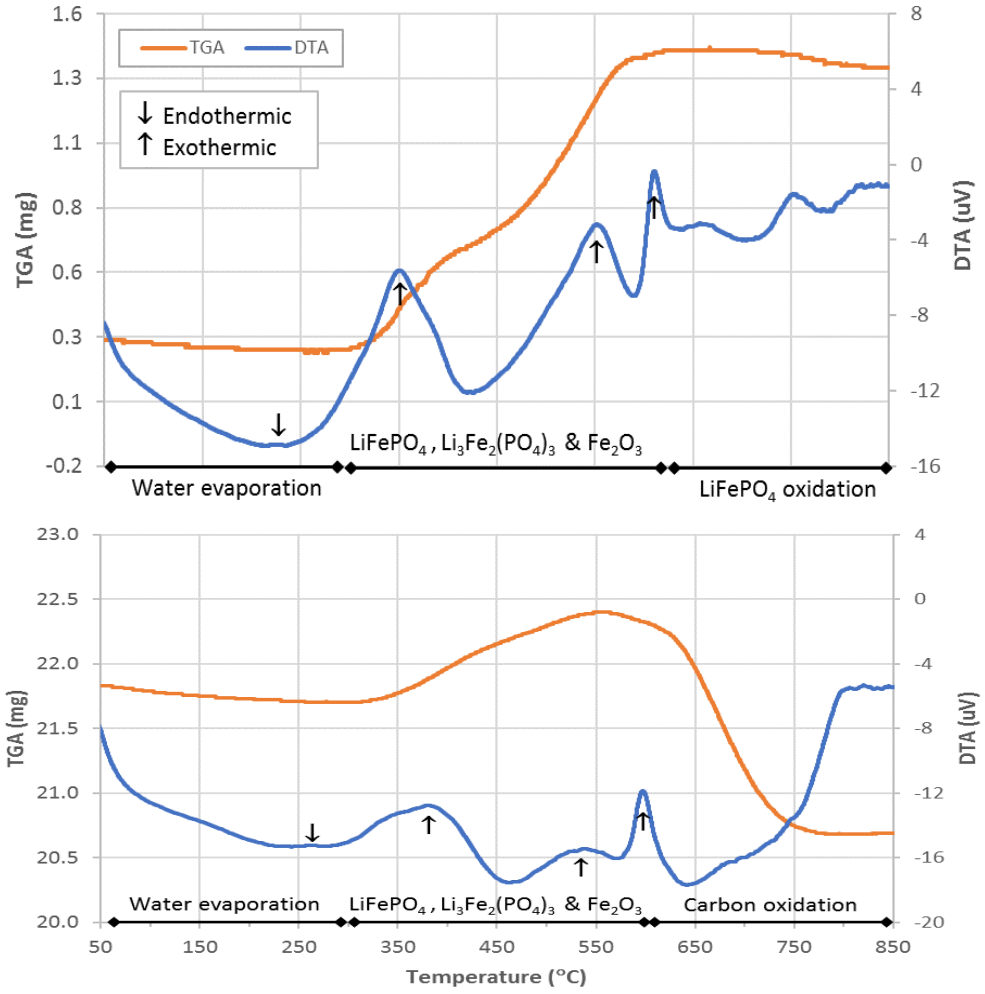

Fig. 1. Thermal analysis curves of (a) $LiFePO_4$ and (b) $LiFePO_4$/C

The next stage is a constant plane with slight weight reduction in order to continues oxidation of $LiFePO_4$. This result is in agreement with that obtain by others in which the olivine $LiFePO_4$ will oxidized into $Li_3Fe_2(PO_4)_3$ and Fe_2O_3 at temperature range of 250-550°C [9], [14], [16] without any other substances that protect $LiFePO_4$, even when 30 mL/min N_2 is still flowing.

Visual observation of $LiFePO_4$/C after thermal characterization shows that most all of the samples were black with a little red on the surface as can be seen in Fig. 1b. The red part could be $Li_3Fe_2(PO_4)_3$ and Fe_2O_3, which occurred as a result of oxidation, whereas the black part would be crystalline $LiFePO_4$. Mass change of the $LiFePO_4$/C curve can also be divided into 3 stages. In the first part, at temperature of 60-300°C, there is a slight decrease in weight due to water evaporation. The second stage occur within the range of 300-510°C. In this stage, the weight increases 1.93%, and two reactions take place. The first reaction is oxidation of $LiFePO_4$ into $Li_3Fe_2(PO_4)_3$ + Fe_2O_3 and the second is decomposition of amorphous $LiFePO_4$ into crystalline $LiFePO_4$ according to the following reaction:

$$C\text{-}LiFe^{II}PO_{4\ (amorphous)} + ¼\ O_2 + nO_2 \rightarrow$$
$$C_{n\text{-}1}\text{-}LiFe^{II}PO_{4\ (crystalline)} + 1/3\ Li_3Fe_2^{III}(PO_4)_3 + 1/6\ Fe_2{}^{III}O_3 + n\ CO_2 \quad (4)$$

The third stage is at 510-750°C, where the weight decreases by 4.8% due to carbon oxidation into CO_2, leaving the $LiFePO_4$ coupled with the excess carbons. The carbon content of $LiFePO_4$/C was calculated in which the remaining carbon is equal to total carbon added minus the burned carbon [9]. In this case, the carbons remained active in the material are 5%-4.8% = 0.2%. From this decomposition behavior, it is clear that the carbon role in the calcination process would be mainly as an oxidation protection of $LiFePO_4$. From the thermal behavior, it can be seen that the formation temperature of $LiFePO_4$ crystal completes at 610°C, followed by

oxidation of carbon that completes at 750°C. This $LiFePO_4$ formation temperature is slightly different from that obtained by Frangers [26] at 550 °C for 12 hours with the addition of carbon less than 5 wt.%, while Belharouak [9] obtained at 450 °C. This difference is expected to be due to the precursors used and the synthesis routes [27].

X-ray diffraction patterns of $LiFePO_4$/C at various temperature and $LiFePO_4$ at 750 °C are shown in Fig. 2. The entire diffraction peaks of $LiFePO_4$/C at various calcination temperatures are in agreement with that of $LiFePO_4$ standard indexed to the orthorhombic Pnma space group (JCPDS No.083-2092). Strong and sharp diffraction peaks indicate that $LiFePO_4$/C sample is highly crystalline. For the sample with no carbon, the peaks shift slightly and are in agreement with that of $LiFePO_4$ standard indexed to the orthorhombic Pnmb space group (JCPDS No.019-0721). The peak difference between $LiFePO_4$ and $LiFePO_4$/C is expected to be due to the presence of carbon. There are no other phases nor other impurities are detected in the XRD diffractograms.

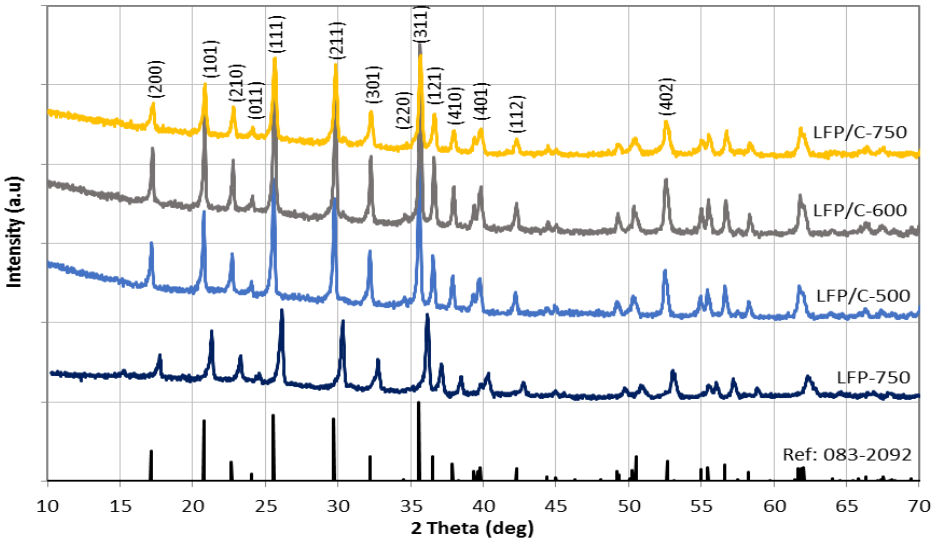

Fig. 2. X-ray diffraction patterns of $LiFePO_4$/C at various calcination temperatures and $LiFePO_4$ at 750 °C.

The variations of unit cell volume (V) and lattice parameters at various calcination temperatures were calculated and the results are summarized in Table 1 and Table 2 for $LiFePO_4$/C and $LiFePO_4$, respectively. At calcination temperature 500ºC, the lattice parameters are in agreement with that reported by other [28] with JCPDS No. 083-2092; however, when the calcination temperature increased to 600 and 700°C, lattice parameters decreased. This could be explained by the facts that at high calcination temperature, more atom carbons will be oxidized forming CO_2 and thus more room for $LiFePO_4$ crystal to get organized and hence the volume gets smaller. The lattice parameters of $LiFePO_4$ are in agreement with that of JCPDS No. 019-0721.

TABLE I $LiFePO_4$/C lattice parameters at different calcination temperatures

Sample	Lattice parameter			
	a (Å)	b (Å)	c (Å)	V (Å^3)
$LiFePO_4$/C-500	10.343	6.004	4.688	291.117
$LiFePO_4$/C-600	10.295	5.991	4.686	289.007
$LiFePO_4$/C-750	10.280	5.996	4.702	289.820
JCPDS 083-2092	10.334	6.010	4.693	291.470

TABLE 2 $LiFePO_4$ lattice parameters at calcination temperature 750 °C

Sample	Lattice parameter			
	a (Å)	b (Å)	c (Å)	V (Å^3)
$LiFePO_4$-750	5.9500	10.196	4.691	291.117
JCPDS 010-0721	5.9970	10.314	4.486	289.840

To understand the effect of carbon addition on the morphology of the $LiFePO_4$/C, secondary electron images using SEM were taken for $LiFePO_4$ and $LiFePO_4$/C from the same calcination temperature of 750°C and the results are shown in Fig. 3. As seen in the figure, $LiFePO_4$ has large grains of up to 10 µm whereas $LiFePO_4$/C has smaller grains (427 nm in average). The large grains size in $LiFePO_4$ is expected to be caused by the grain

growth during calcination. During calcination process, the heat will cause the small grains to merge with the large one by grain boundaries diffusion. The small grain in $LiFePO_4$/C, on the other hand, is expected to be the result of mechanical grinding process, which breaks the precursor grain during the mixing of carbon black and $LiFePO_4$. The carbons then cover the $LiFePO_4$ particles and protect them from grain growth during the calcination process.

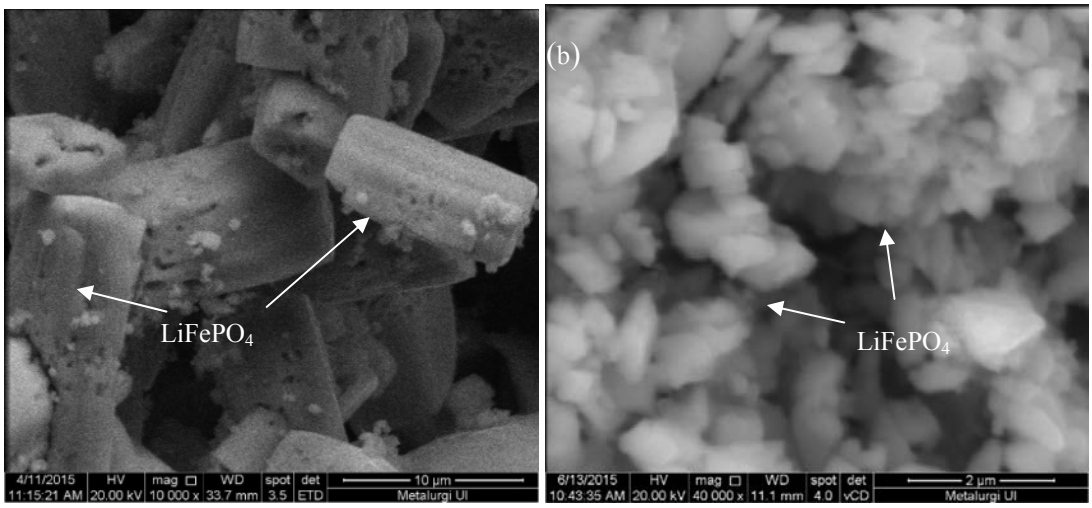

Fig. 3. Secondary electron images of the samples after calcination at 750°C (a) LiFePO4 and (b) LiFePO4/C.

Morphology of $LiFePO_4$/C at different calcination temperatures is shown in Fig. 4. At temperature of 500ºC, $LiFePO_4$/C formed in two shapes i.e. flakes and spheres as shown in Fig 4(a). Flake shaped $LiFePO_4$/C is basically the original shape of $LiFePO_4$ coated by carbon, whereas the sphere one is initiated by the carbon excess. EDX analysis of the flake shape showed that the composition of O = 35.88; P = 23.41 and Fe = 40.71 wt.%, which represents $LiFePO_4$ and sphere composition is dominated by C = 53.72 with the remaining are O = 30.63; P = 05.08; and Fe = 10.57 wt.%. Referring to the $LiFePO_4$/C TGA result shown previously, it can be inferred that at 500ºC, $LiFePO_4$ formation has finished but still contain most of the added carbon. When calcination temperature is increased from 500 to 600ºC, globular shape of carbon disappears because most of the carbons have turned into CO_2 whereas the other carbons agglomerate in the forms of small particles. Furthermore, flake shaped of $LiFePO_4$/C is now dominating the grains. At the calcination temperature 750ºC, only flake shaped $LiFePO_4$ remains coated by carbons on the surface.

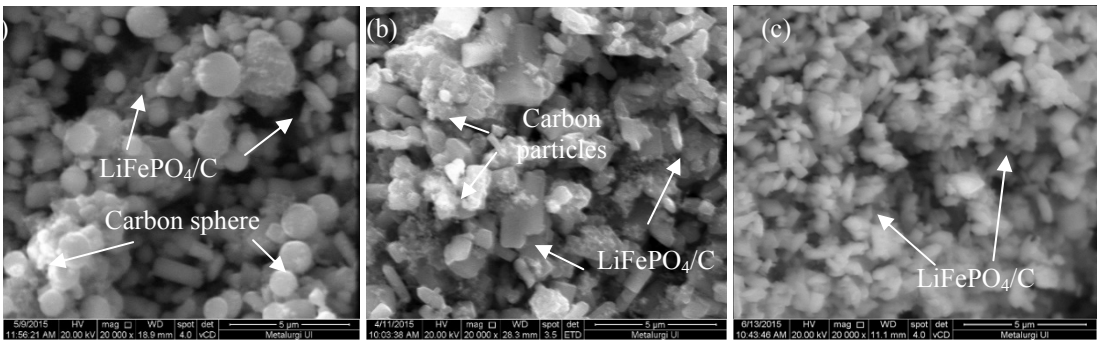

Fig. 4. Secondary electron images of $LiFePO_4$/C calcined at (a) 500°C (b) 600°C and (c) 750°C.

Image analysis has been performed in order to calculate the particle size distribution, and the result is shown in Table 3. Within temperature increment from 500 to 600ºC, grain growth occurs in $LiFePO_4$/C flake and make the size of the flake to become large although it is not as large as pure $LiFePO_4$. This can be understood since the grain growth mechanism will occur when two grain boundaries in same phase but different size get into contact each other. In this case, carbon will act as a barrier that keeps $LiFePO_4$ grain boundary from being contacted. At temperature 750ºC, the grain size is supposed to be larger than that of lower temperature. In this case, however, it turns to be small. This is expected because of the effect of mechanical mixing before calcination, and thus the carbon sphere disappears in this temperature. This confirm the result of DTA-TGA curve where the carbon oxidation has completed at 750ºC. Hydrothermal synthesis followed by calcination process without additional carbon is indeed susceptible to grain growth. This confirms that the carbons act as inhibiting additive for the grain growth [15].

TABLE 3. Averaged particle size of LiFePO4/C and LIFEPO$_4$ after calcination

Sample	Flake width (nm)	Flake length(nm)	Carbon Sphere (nm)
LiFePO$_4$/C-500	51	572	629
LiFePO$_4$/C-600	68	664	114 (agglomerated)
LiFePO$_4$/C-750	80	427	-
LiFePO$_4$-750	3000	10536	-

The effect of carbon addition and calcination temperature on the electrical conductivity of crystalline LiFePO$_4$ was examined from pressed LiFePO$_4$/C and LiFePO$_4$ sample pellets using EIS. The conductivity test result is shown in Table 4. Pure LiFePO$_4$ crystal is having insulator property, and thus the test result of LiFePO$_4$ shows only a conductivity in the order of 10^{-7} S/cm. This result is in agreement with other results [3], [12]. With the addition of carbon, the conductivity increases. In this instance, carbon will act as a conductive agent, and hence, more carbon will increase the conductivity. Conductivity, however, reduces at increasing calcination temperature as shown in Table 4. As has been mentioned previously, at high calcination temperature, more atom carbon will oxidize to form CO_2 and thus less carbon will be available to cover the LiFePO$_4$.

TABLE 4 Electrical conductivity test result

Sample	Conductivity (S/cm)
LiFePO$_4$/C-500	1.072×10^{-2}
LiFePO$_4$/C-600	7.063×10^{-3}
LiFePO$_4$/C-750	2.231×10^{-4}
LiFePO$_4$-750	5.009×10^{-7}

The conductivity of active material is also related to the particle size, as shown in Fig.5. With the assumption that the flake size is proportional to the grain size, whereas the electron will take the shortest path to travel, the electrical conductivity will be lower at larger particle size. This can be understood since the larger the particle sizes the greater the distance and thus the lower the conductivity.

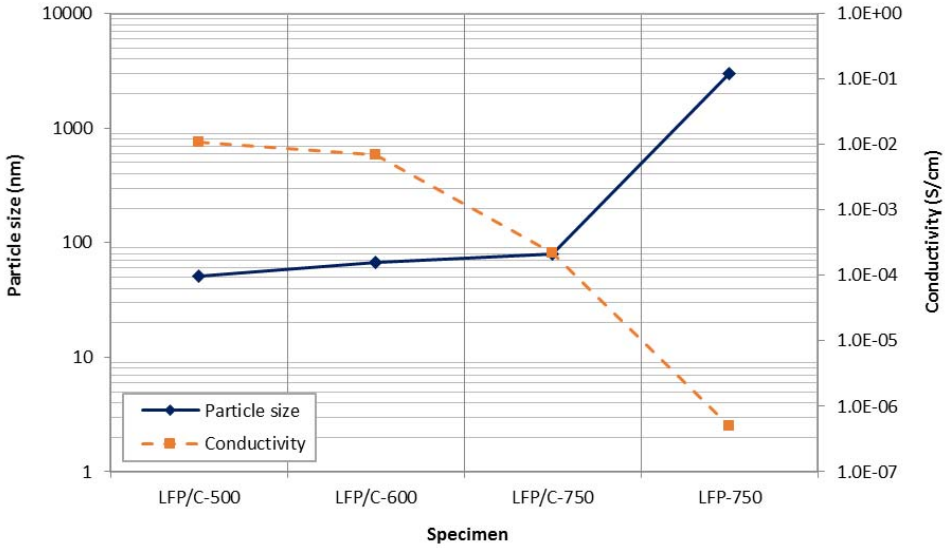

Fig. 5. Relationship between particle size and electrical conductivity in LiFePO4/C

In order to determine the capacity and performance of LiFePO$_4$ cathode, charge–discharge cycle tests were performed on LiFePO$_4$/C at various rates. Result from LiFePO$_4$/C sample showed that the stable active material is the sample with carbon addition and calcined at 750°C. The charge–discharge voltage curves for the LiFePO$_4$/C-750 in the voltage range of 2.5–4.0 volts and current density of 0.1-0.5C are shown in Fig. 6. A flat profile over 3.3–3.5 volts potential range indicates that the extraction and the insertion reaction of the lithium ions proceeded by the motion of a two-phase interface between FePO$_4$ and LiFePO$_4$. The specific capacity from the testing that yet to be improved is at 11.66 mAh/g for 0.1C. This low value could be due to hygroscopic properties of carbon, which allows it to get very high absorption rate of water vapor. The water content and

other contaminants could reduce the capacity and damage the electrolyte solution and the cathode [17], [22]. Nonetheless, despite the low capacity, the trend obtained in this work is promising for the next development.

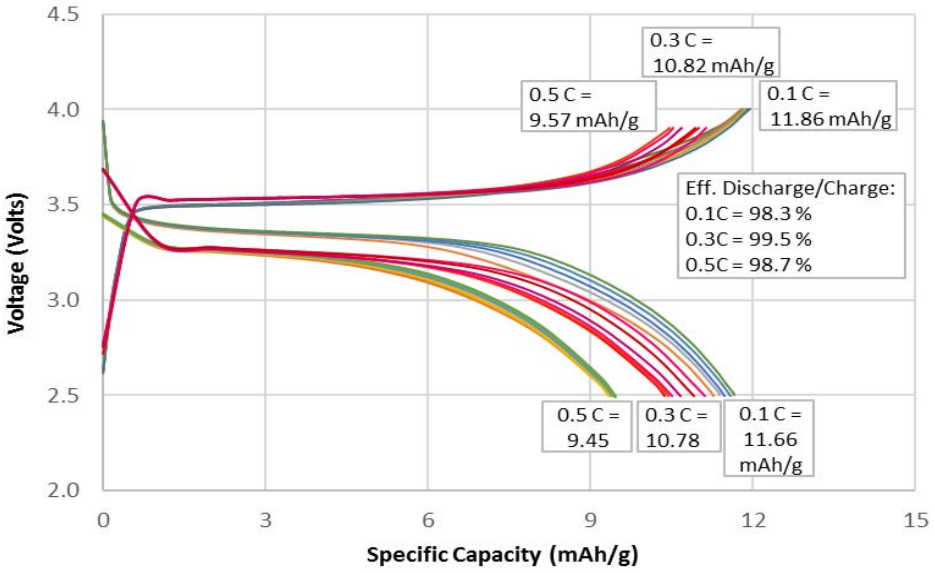

Fig. 6. Charge/discharge test results in the potential range of 2.5–4.0 volts at room temperature for the $LiFePO_4$/C calcined at 750 °C.

IV. Conclusion

Pure $LiFePO_4$ and carbon coated $LiFePO_4$ has been synthesized using hydrothermal route. Thermal decomposition behaviour showed that $LiFePO_4$ formation was completed at 510°C followed by carbon oxidation until 750°C. The addition of carbon effectively protected the material from oxidation and grain growth during calcination process. High calcination temperature resulted in large grain particles and reduction of carbon content. The X-ray diffraction diffractograms exhibited well crystallized peaks corresponding to an orthorhombic olivine type structure with Pnma space group. SEM analysis showed that the synthesized powder consists of flake-like shaped grains in the size range of 400–650 nm. The charge-discharge measurements performed at various rates exhibited a good cycling stability under working voltage at 3.3~3.5 volts.

Acknowledgement

The authors would like to express their gratitude to the Directorate of Research and Community Services (DRPM) Universitas Indonesia and Science and Technology Centre for Advanced Materials, National Nuclear Energy Agency (BATAN), Indonesia. Publication of the paper is supported in part by Hibah PITTA No. 822/UN2.R3.1/HKP.05.00/2017.

References

[1] A. K. Padhi, K. S. Nanjundaswamy, J. Goodenough, "Phospho-olivines as Positive-Electrode Materials for Rechargeable Lithium Batteries," Electrochem. Soc., vol. 144, No.4, p. 1188-1195, 1997.
[2] L-H. Hu, F. Y. Wu, C. T. Lin, A. N. Khlobystov, L. J. Li, "Graphene-modified $LiFePO_4$ cathode for lithium ion battery beyond theoretical capacity," Nature Commun., vol. 4 No. 1687, pp. 1-7, 2013.
[3] S. Y. Chung, J. T. Bloking, Y.M. Chiang, "Electronically conductive phospho-olivines as lithium storage electrodes," Nat. Mater., vol. 1, pp. 123-128, 2002.
[4] J. Lim, S-W. Kang, J. Moon, S. Kim, H. Park, J. P. Baboo, J. Kim, "Low-temperature synthesis of $LiFePO_4$ nanocrystals by solvothermal route," Nanoscale Res. Lett. vol. 7 No. 3, pp. 1-7, 2012.
[5] W. Yu, L. Wu, J. Zhao, Y. Zhang, G. Li, "Synthesis of $LiFePO_4$/C nanocomposites via ionic liquid assisted hydrothermal method," J. Electroanal. Chem. Vol. 704, pp. 214-219, 2013.
[6] D. Arumugam, G. P. Kalaignan, P. Manisankar, "Synthesis and electrochemical characterizations of nano-crystalline $LiFePO_4$ and Mg-doped $LiFePO_4$ cathode materials for rechargeable lithium-ion batteries," J. Solid State Electrochem., vol. 13 No. 2, pp. 301-307, 2008.
[7] H. Liu, J. Xie, K. Wang, "Synthesis and characterization of $LiFePO_4$/(C+Fe_2P) composite cathodes," Solid State Ionics, vol. 179, No. 27-32, pp. 1768-1771, 2008.
[8] R. Dominko, M. Bele, M. Gaberscek, M. Remskar, D. Hanzel, S. Pejovnik, J. Jamnik, "Impact of the Carbon Coating Thickness on the Electrochemical Performance of $LiFePO_4$/C Composites," J. Electrochem. Soc., vol. 152 No. 3, pp. A607-A610, 2005.
[9] I. Belharouak, C. Johnson, K. Amine, "Synthesis and electrochemical analysis of vapor-deposited carbon-coated $LiFePO_4$," Electrochem. Commun., vol. 7 No. 10, pp. 983-988, 2005.
[10] Z.P. Guo, H. Liu, S. Bewlaya, H.K. Liu, S.X. Dou, "A New Synthetic Method for Preparing LiFePO4 with Enhanced Electrochemical Performance," J. New Mat. Electrochem. Systems, vol. 6, pp. 259-262, 2003.
[11] X. Sun, K. Sun, C. Chen, H. Sun, B. Cui, "Controlled Preparation and Surface Structure Characterization of Carbon-Coated Lithium Iron Phosphate and Electrochemical Studies as Cathode Materials for Lithium Ion Battery," Int. J. Mater. Chem., vol. 2 No. 5, pp. 218-224, 2013.
[12] K-F. Hsu, S-Y. Tsay, B-J. Hwang, "Synthesis and characterization of nano-sized LiFePO4 cathode materials prepared by a citric acid-based sol-gel route," J. Mater. Chem., vol. 14 No. 17, pp. 2690-2695, 2004.

[13] J. Yang, J. J. Xu, "Nonaqueous Sol-Gel Synthesis of High-Performance $LiFePO_4$," Electrochem. Solid State Lett., vol. 7 No. 12, pp. A515-A518, 2004.
[14] H-G. Deng, S-L. Jin, X. He, L. Zhan, W-M. Qiao, L-C. Ling, "$LiFePO_4$/C Nanocomposites Synthesized from Fe_2O_3 by a Hydrothermal Reaction-Calcination Process and Their Electrochemical Performance," J. Inorg. Mater., vol. 27 No. 9, pp. 997-1002, 2012.
[15] M. Mazman, Ö. Çuhadar, D. Uzun, E. Avci, E. Biçer, T. C. Kaypmaz, Ü. Kadiroğlu, "Optimization of LiFePO4 synthesis by hydrothermal method," Turk. J. Chem., vol. 38, pp. 297-308, 2014.
[16] Q. Tan, C. Lv, Y. Xu, J. Yang, "Mesoporous composite of $LiFePO_4$ and carbon microspheres as positive-electrode materials for lithium-ion batteries," Particuology, vol. 17, pp. 106-113, 2014.
[17] J. Wang, Y. Tang, J. Yang, R. Li, G. Liang, X. Sun, "Nature of $LiFePO_4$ aging process: Roles of impurity phases," J. Power Sources, vol. 238, pp. 454-463, 2013.
[18] W. Yu, L. Wu, J. Zhao, Y. Zhang, G. Li, "Synthesis of $LiFePO_4$/C nanocomposites via ionic liquid assisted hydrothermal method," J. Electroanal. Chem., vol. 704, p. 214-219, 2013.
[19] N. Zhou, H-Y. Wang, E. Uchaker, M. Zhang, S-Q. Liu, Y-N. Liu, G. Cao, "Additive-free solvothermal synthesis and Li-ion intercalation properties of dumbbell-shaped $LiFePO_4$/C mesocrystals," J. Power Sources, vol. 239, pp. 103-110, 2013.
[20] M-Y. Cho, K-B. Kim, J-W. Lee, H. Kim, H. Kim, K. Kang, K. C. Roh, "Defect-free solvothermally assisted synthesis of microspherical mesoporous LiFePO4/C," RSC Adv., vol. 3 No. 10, pp. 3421-3427, 2013.
[21] X. Sun, K. Sun, Y. Wang, X. Bai, C. Chen, B. Cui, "Scale-up synthesis, Structure Characterization and Electrochemical Characteristics of C-$LiFePO_4$ Nanocomposites for Lithium Ion Rechargeable Batteries," Int. J. Electrochem. Sci. 8, pp. 12816-12836, 2013.
[22] J-F. Martin, M. Cuisinier, N. Dupré, A. Yamada, R. Kanno, D. Guyomard, "More on the reactivity of olivine $LiFePO_4$ nano-particles with atmosphere at moderate temperature," J. Power Sources, vol. 196 No. 4, pp. 2155-2163, 2011.
[23] K. Shiraishi, K. Dokko, K. Kanamura, "Formation of impurities on phospho-olivine $LiFePO_4$ during hydrothermal synthesis," J. Power Sources, vol. 146 No. 1-2, pp. 555-558, 2005.
[24] X. Ou, G. Liang, L. Wang, S. Xu, X. Zhao, "Effects of magnesium doping on electronic conductivity and electrochemical properties of LiFePO4 prepared via hydrothermal route," J. Power Sources, vol. 184, pp. 543-547, 2008.
[25] L-H. He, Z-W. Zhao, X-H. Liu, A-L. Chen, X-F. Si, "Thermodynamics analysis of LiFePO4 pecipitation from Li–Fe(II)–P–H_2O system at 298 K," Trans. Nonferrous Met. Soc. China, vol. 22 No. 7, pp. 1766-1770, 2012.
[26] S. Franger, F. Le Cras, C. Bourbon, H. Rouault, "Comparison between different $LiFePO_4$ synthesis routes and their influence on its physico-chemical properties," J. Power Sources, vol. 119-121, pp. 252-257, 2003.
[27] N. Sofyan, D.Y. Putro, A. Zulfia, "Performance of Vanadium-Doped $LiFePO_4$/C Used as Cathode for Lithium Ion Battery," Int. J. Technol., vol. 7 No. 8, pp. 1307-1315, 2016.
[28] J. Popovic, "Novel lithium iron phosphate materials for lithium-ion batteries," Dissertation, University of Potsdam, 2011.

AUTHOR PROFILE

Nofrijon Sofyan is an Associate Professor at the Department of Metallurgical and Materials Engineering, Universitas Indonesia. He obtained his B.Sc. in Chemistry from Andalas University, Padang, 1992, and M.Sc. in Materials Science from Universitas Indonesia, Jakarta, 1997. He received his Ph.D. in Materials Engineering from Auburn University, USA, 2008. His research areas include nanomaterials, dye-sensitized solar cells, lithium ion batteries, and superconductors.

Guntur Tri Setiadanu is an Engineer at Research Center for Electricity Technology Development, New and Renewable Energy and Energy Conservation, Ministry of Energy and Mineral Resources. He received his Bachelor of Engineering from Department of Mechanical Engineering, Gadjah Mada University, Yogyakarta, 2003. He received his M.Eng. in Metallurgical and Materials Engineering, Universitas Indonesia, 2014.

Anne Zulfia is a Professor at the Department of Metallurgical and Materials Engineering, Universitas Indonesia. She obtained her B.Eng. in Metallurgical Engineering from Universitas Indonesia. She received her Masters and Ph.D. from Department of Engineering Materials, University of Sheffield, United Kingdom. Her research areas include nanocomposite materials and lithium ion batteries.

Evvy Kartini is a Research Professor at National Nuclear Energy Agency, Republic of Indonesia. She is an expert on the neutron scattering and solid state ionic. She began her research on Superionic glasses early 1990, at Hahn Meitner Institute, Berlin, Germany. The existence of Boson peaks in $ZnCl_2$ and CKN glasses were an interesting phenomenon, therefore she conducted experiment on inelastic neutron scattering at Nuclear Research Reactor, Chalk River Laboratory, Canada. In 1995-1996, she returned to Germany, and finished her PhD at the Technical University (TU), Berlin, Germany. During this period, she was also had a chance to attend a precious course "Higher European Research Course for Users Using Large System (HERCULES)" in Institute of Laue Langevin, Grenoble, France and other nuclear facilities in France. Her research of interests is in Condensed Matter, Physics, Materials Science, and Neutron Scattering.